Annals of Nuclear Medicine Vol. 19, No. 6, 469–477, 2005

Usefulness of noise adaptive non-linear Gaussian filter in FDG-PET study

Makoto NAGAYOSHI,*,** Kenya MURASE,* Kouichi FUJINO,** Yusuke UENISHI,* Minoru KAWAMATA,*
Yukio NAKAMURA,** Keishi KITAMURA,*** Ichiro HIGUCHI,**** Naohiko OKU**** and Jun HATAZAWA****

*Department of Medical Physics and Engineering, Graduate School of Medicine, Osaka University
**Department of Radiology, Osaka University Hospital
***R & D Department, Medical Systems Division, Shimadzu Corporation
****Department of Tracer Kinetics, Graduate School of Medicine, Osaka University

Objective: In positron emission tomography (PET) studies, shortening transmission (TR) scan time can improve patient comfort and increase scanner throughput. However, PET images from short TR scans may be degraded due to the statistical noise included in the TR image. The purpose of this study was to apply non-linear Gaussian (NLG) and noise adaptive NLG (ANLG) filters to TR images, and to evaluate the extent of noise reduction by the ANLG filter in comparison with that by the NLG filter using phantom and clinical studies. ***Methods:*** In phantom studies, pool phantoms of various diameters and injected doses of 2-deoxy-2-[^{18}F]fluoro-D-glucose (FDG) were used and the coefficients of variation (CVs) of the counts in the TR images processed with the NLG and ANLG filters were compared. In clinical studies, two normal volunteers and 13 patients with tumors were studied. In volunteer studies, the CV values in the liver were compared. In patient studies, the standardized uptake values (SUVs) of tumors in the emission images were obtained after processing the TR images using the NLG and ANLG filters. ***Results:*** In phantom studies, the CV values in the TR images processed with the ANLG filter were smaller than those in the images processed with the NLG filter. When using the ANLG filter, their dependency on the phantom size, injected dose of FDG and TR scan time was smaller than when using the NLG filter. In volunteer studies, the CV values in the images processed with the ANLG filter were smaller than those in the images processed with the NLG filter, and were almost constant regardless of the TR scan time. In patient studies, there was an excellent correlation between the SUVs obtained from the images with a TR scan time of 7 min processed with the NLG filter (x) and those obtained from the images with a TR scan time of 4 min processed with the ANLG filter (y) ($r = 0.995$, $y = 1.034x - 0.075$). ***Conclusions:*** Our results suggest that the ANLG filter is effective and useful for noise reduction in TR images and shortening TR scan time while maintaining the quantitative accuracy of FDG-PET studies.

Key words: positron emission tomography, 2-deoxy-2-[^{18}F]fluoro-D-glucose, non-linear Gaussian filter, noise adaptive non-linear Gaussian filter, transmission scan

INTRODUCTION

POSITRON EMISSION TOMOGRAPHY (PET) studies using 2-deoxy-2-[^{18}F]fluoro-D-glucose (^{18}F-FDG) (FDG-PET) can measure glucose metabolism, and are useful for diagnosing, staging, and restaging the most important cancers and for monitoring various cancer treatments.[1]

For the quantitative measurement of radioactivities using PET, attenuation correction using transmission scanning is required. In PET studies, shortening the transmission scan time can improve patient comfort and increase scanner throughput. However, short transmission scans apparently cause an increase of statistical noise in transmission images, which may propagate into the reconstructed PET images.

The non-linear Gaussian (NLG) filter[2–4] has been

Received February 7, 2005, revision accepted June 3, 2005.

For reprint contact: Kenya Murase, Ph.D., Department of Medical Physics and Engineering, Division of Medical Technology and Science, Course of Health Science, Graduate School of Medicine, Osaka University, 1–7 Yamadaoka, Suita, Osaka 565–0871, JAPAN.

E-mail: murase@sahs.med.osaka-u.ac.jp

applied to reduce the statistical noise in transmission images. However, the NLG filter is not sufficient to reduce the statistical noise in transmission images when the transmission scan time is short. Recently, the noise adaptive non-linear Gaussian (ANLG) filter has been developed and is suggested to reduce the statistical noise in transmission images more effectively than the NLG filter.[5] The purpose of this study was to apply the NLG and ANLG filters to transmission images and to evaluate the extent of noise reduction by the ANLG filter and the usefulness of the ANLG filter in FDG-PET studies in comparison with the NLG filter using phantom and clinical studies.

MATERIALS AND METHODS

Non-linear Gaussian filter

For an image with value $f(p)$ at pixel p, a linear Gaussian filter operation is defined by

$$G_g \cdot f(p) = \frac{1}{N_p} \sum_{q \in D} \phi_g(p - q) f(q), \quad (1)$$

where

$$N_p = \sum_{q \in D} \phi_g(p - q),$$

and

$$\phi_g(t) = \exp(-t^2/2g^2).$$

D denotes a certain window of neighboring pixels centered at p, and g determines the effective window width.

In this type of smoothing operation, which is essentially a local weighted average in the neighborhood, using a smaller window can lessen edge-blurring effects but also lessens noise reduction capabilities. In order to preserve edges, the influence of $f(q)$ should decrease when the difference in pixel values $|f(p) - f(q)|$ increases. This can be achieved by introducing an additional weight $\phi_h(f(p) - f(q))$. Thus, the NLG filter operation is defined by[2–4]:

$$G_{g,h} \cdot f(p) = \frac{1}{N_p} \sum_{q \in D} \phi_g(p - q) \phi_h(f(p) - f(q)) f(q), \quad (2)$$

where

$$N_p = \sum_{q \in D} \phi_g(p - q) \phi_h(f(p) - f(q)),$$

$$\phi_g(t) = \exp(-t^2/2g^2),$$

and

$$\phi_h(t) = \exp(-t^2/2h^2).$$

g and h are smoothing parameters measuring the width of ϕ_g and ϕ_h, respectively.

For sufficient smoothing, several filtering steps with different parameters are performed. The parameter g of the first step should be as small as possible in order to avoid unnecessary blurring of coarser structures, but also as large as the size of fine structures. The parameter h of the first step should be determined based on the maximal contrast of the fine structures which finally have to be eliminated. To make the following filter steps sharpen the edges of the coarser structures, g has to be increased and h has to be decreased. In the last step, the final weights are calculated using the current image and applied to the original image $f_0(p)$ to maintain the corresponding local averages of the original image. This modified filtering step is defined as follows:

$$G_{g,h} \cdot f_0(p) = \frac{1}{N_p} \sum_{q \in D} \phi_g(p - q) \phi_h(f(p) - f(q)) f_0(q). \quad (3)$$

Currently, the smoothing parameters g and h and the number of filtering steps are determined empirically.[4] In this study, they were taken as 4.65 mm, 0.032 cm^{-1} and 3, respectively.

Noise adaptive non-linear Gaussian filter

The filter kernel of the NLG filter is the product of the weight on the difference in pixel locations and the weight on the difference in attenuation values. The parameter of the latter weight is thought to be dependent on the noise level of the transmission image, and needs to be optimized according to the transmission count. Thus, the ANLG filter, in which the filter parameters are automatically determined with the estimated variance in transmission images, was investigated.

As previously described, for a transmission image with value $f(p)$ at pixel p, the NLG filter is defined by Eq. (2). For sufficient smoothing, several filtering steps with different parameters (g and h) are performed as follows:

$$g_{i+1} = 2g_i \text{ and } h_{i+1} = h_i/2, \quad (4)$$

for the ith filtering step. In this study, the number of filtering steps was taken as 3 as in the NLG filter. The initial value of the parameter g (g_0) was set to be as small as possible in order to avoid unnecessary blurring of coarser structures. In this study, g_0 was taken as 2 mm. On the other hand, the initial value of the parameter h (h_0) was determined based on the local image noise variance var(p) estimated individually from the measured transmission projections at each pixel position:

$$h_0(p) = 3\sqrt{\text{var}(p)}, \quad (5)$$

where the coefficient of 3 was used in order to eliminate as much spike noise as possible.[3]

The local image variances var(p) were estimated from the measured transmission sinograms by the following formula[6]:

$$\text{var}\{p(x,y)\} = c \sum_{\phi} \int \text{filter}(s' - s)^2 \frac{1}{N_0} e^{t(s,\phi)} ds, \quad (6)$$

where $s' = x \cos\phi + y \sin\phi$, N_0 is the number of incident photons in transmission, $t(s,\phi)$ is a transmission sinogram,

and filter indicates a reconstruction filter kernel. The scale factor c was calculated by the ratio of variances in the peripheral region of transmission images with an attenuation coefficient of zero.

Whereas a filter chain does not displace edges it may happen that the values of the filter chain output in the regions between the edges differ slightly from the corresponding local averages of the original image. This can be avoided by appending a modified filter step, and smoothes the original image while respecting the edges present in the filter chain output.[2]

Figures 1 (a) and 1 (b) show the flowchart of the NLG filtering method and that of the ANLG filtering method, respectively.

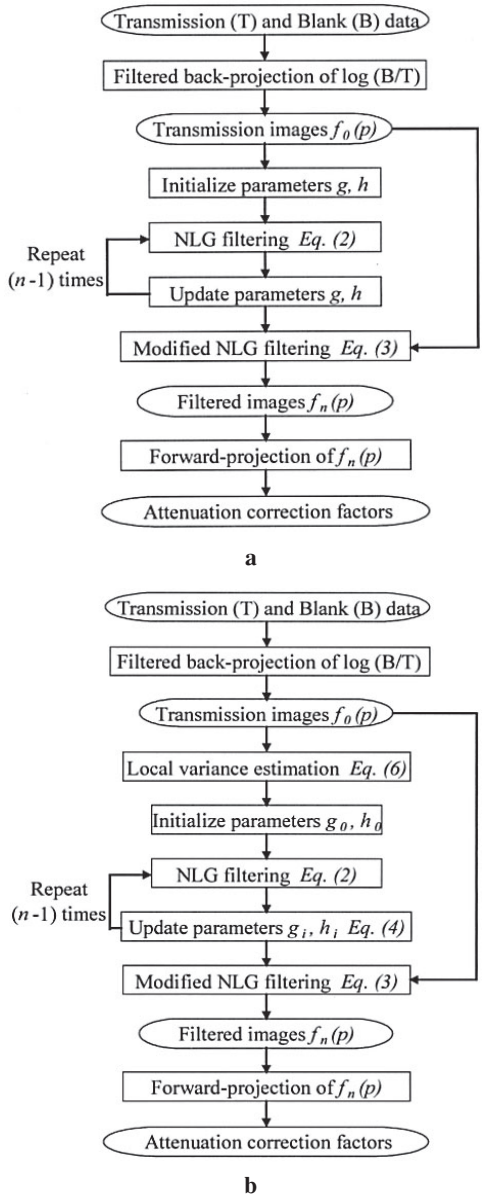

Fig. 1 Flowcharts of the non-linear Gaussian (NLG) filtering method (a) and the noise adaptive non-linear Gaussian (ANLG) filtering method (b).

Reconstruction of transmission image

Transmission projection data were smoothed using a 2-dimensional linear Gaussian filter with a full width at half maximum (FWHM) of 1.5 pixels in order to avoid zero division in the calculation of logarithms between blank and transmission sinograms. The transmission image was then reconstructed from transmission projection data into a 128 × 128 matrix with a pixel size of 4 mm using the filtered back-projection (FBP) method with Shepp-Logan filter[7] of Nyquist frequency cutoff.

Reconstruction of emission image

The emission image was reconstructed from emission projection data into a 128 × 128 matrix with a pixel size of 4 mm using the ordered subset-expectation maximization (OS-EM) algorithm[8] in which the numbers of subsets and iterations were taken as 6 and 4, respectively, and the transmission image obtained above was used as an attenuation coefficient map.

Phantom study

All measured data were acquired with a Headtome-V (SET-2300W) PET scanner (Shimadzu Corp., Kyoto, Japan) with 590-mm axial field of view (FOV) and 63 slices. A simultaneous emission and transmission (SET) scan protocol[9,10] was used for data acquisition. Transmission scan time varied from 30 sec to 15 min, while emission scan time was fixed at 15 min. To investigate the capability of noise reduction of the NLG and ANLG filters, transmission data were extracted by separating transmission and emission data from SET data.[9,10] Since the injected dose of ^{18}F-FDG and phantom size may influence the quality of transmission images in the case of short transmission scan time, we investigated these effects by varying them in the phantom studies.

Effect of phantom size

To investigate the effect of phantom size, three pool phantoms with different inner diameters (16, 20 and 27 cm) containing ^{18}F-FDG aqueous solution of 55.5 MBq were used for various transmission scan times. The region of interest (ROI) was drawn on the center of the transaxial transmission images of the phantom as illustrated in

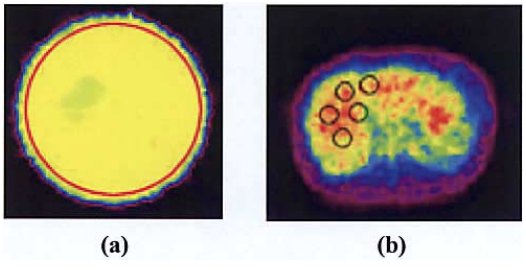

Fig. 2 (a) Region of interest (ROI) drawn on the transmission image of a pool phantom. (b) ROIs drawn on the liver region in the transmission image of a volunteer.

Table 1 Characteristics of the patients used in clinical studies

Patient No.	Gender	Age (years)	Body weight (kg)	Injected dose of ^{18}F-FDG (MBq)	Diagnosis
1	F	54	64.0	339.7	Retroperitoneum leiomyosarcoma
2	M	28	72.0	382.6	Testicular malignant tumor
3	M	78	62.0	373.3	Lung cancer
4	M	54	80.0	516.5	Esophageal cancer
5	M	63	53.0	377.4	Esophageal cancer
6	M	77	56.5	375.6	Gastric cancer
7	M	54	67.5	352.6	Pancreas cancer
8	M	56	50.0	325.6	Esophageal cancer
9	M	47	65.0	390.7	Para aortic tumor
10	M	50	69.0	397.0	Rectum cancer
11	F	53	42.0	316.7	Esophageal cancer
12	M	73	45.0	357.4	Esophageal cancer
13	M	63	53.0	377.4	Lung cancer

^{18}F-FDG, 2-deoxy-2-[^{18}F]fluoro-D-glucose; F, female; M, male.

Figure 2 (a). The mean and standard deviation (SD) of the counts in each ROI were obtained, and the coefficient of variation (CV) was calculated from SD/mean × 100 (%). We compared the CV values in the transmission images processed with the NLG and ANLG filters, and visually compared the image quality of their emission images.

Effect of the injected dose of ^{18}F-FDG

To investigate the effect of the injected dose of ^{18}F-FDG, a pool phantom with an inner diameter of 20 cm was filled with four quantities of ^{18}F-FDG (18.5, 37, 74 and 111 MBq). The ROI was drawn on the center of the transaxial transmission images of the phantom. The mean and SD of the counts in each ROI were obtained, and the CV value was calculated from SD/mean × 100 (%) as described above. We compared the CV values in the transmission images processed with the NLG and ANLG filters, and visually compared the quality of the emission images.

Clinical study

To investigate the effectiveness and usefulness of the ANLG filter for noise reduction and tumor detection in comparison with the NLG filter for short transmission scan time, two normal volunteers (body weight, 67.5 ± 9.2 kg; age, 35.0 ± 9.9 years) and thirteen patients with tumors (body weight, 60.5 ± 11.4 kg; age, 57.3 ± 14.0 years) were studied with FDG-PET. The body mass indices (BMI) of volunteers A and B were 20.2 and 25.3, respectively. Table 1 summarizes the characteristics of the patients. Informed consent was obtained from each participant after a detailed explanation of the purpose of the study and the scanning procedures.

In the normal volunteer study, the protocol for SET scans[9,10] was used. The transmission scan time was varied from 1 to 16 min in a power of two such as 1, 2, 4, 8 and 16 min, while the emission scan time was fixed at 8 min. The ROIs were drawn on the liver in the transaxial emission images as illustrated in Figure 2 (b). The mean and SD of the counts in the ROI were obtained, and then the CV values were calculated as previously described.

In the patient study, the protocol for SET scans[9,10] was also used. The transmission scan time was set at 4 min and 7 min, while the emission scan time was fixed at 7 min. These scan times have been routinely used in our clinical setting. It should be noted that the emission scan time in the patient study was shorter by 1 min than that in the normal volunteer study. To investigate the effect of the transmission scan time on the quantitative accuracy of FDG-PET studies, the standardized uptake value (SUV) was calculated for each tumor. The SUV was determined as the average radioactivity in the tissue divided by the injected dose normalized by the body weight. Thus, the SUV was calculated according to the following formula:

$$\mathrm{SUV} = \frac{\text{concentration in tissue (Bq/g)}}{\text{injected dose (Bq)/body weight (g)}} . \quad (7)$$

The ROIs were placed on the tumor regions. Three SUVs (SUV [NLG (7 min)], SUV [ANLG (7 min)] and SUV [ANLG (4 min)]) were calculated for each tumor. SUV [NLG (7 min)] represents the SUV obtained from the emission image in which the transmission image with a scan time of 7 min was processed using the NLG filter. SUV [ANLG (7 min)] and SUV [ANLG (4 min)] represent the SUV obtained from the emission image in which the transmission image was processed using the ANLG filter with transmission scan times of 7 min and 4 min, respectively.

RESULTS

Phantom study

Figure 3 shows the CV values in the transmission images of the pool phantoms with various diameters as a function

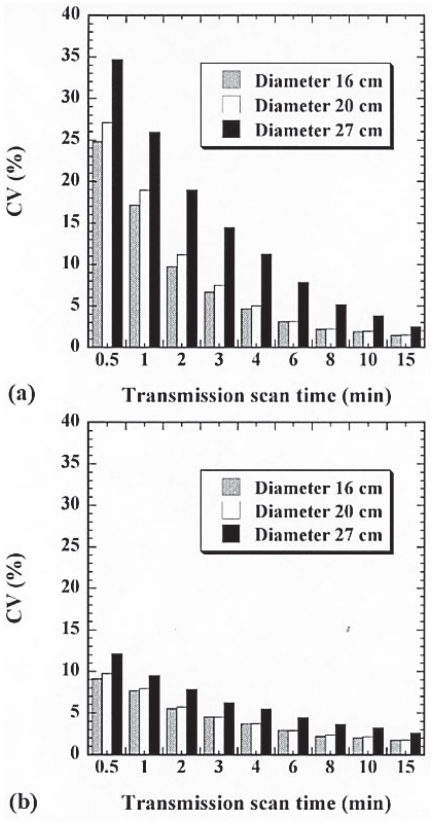

Fig. 3 Coefficient of variation (CV) values in the transmission images processed by NLG (a) and ANLG filters (b) as a function of transmission scan time for pool phantoms with various diameters.

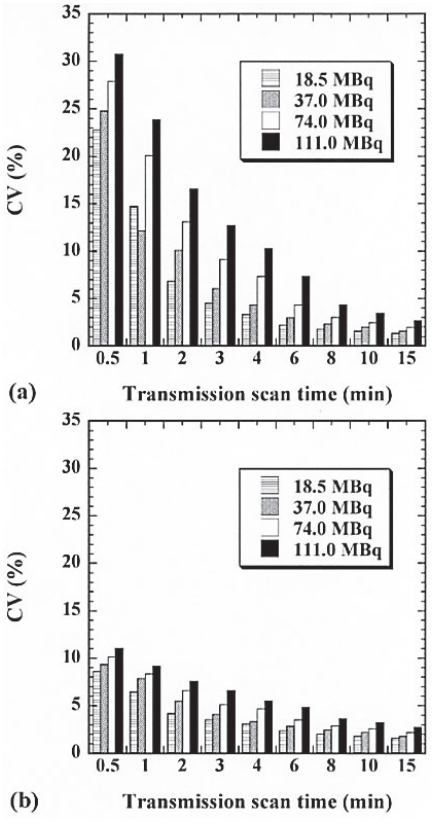

Fig. 4 CV values in the transmission images processed with the NLG (a) and ALNG filters (b) as a function of transmission scan time for the pool phantoms with various injected doses of 2-deoxy-2-[^{18}F]fluoro-D-glucose (^{18}F-FDG).

of transmission scan time. Figures 3 (a) and 3 (b) show cases using the NLG and ANLG filters, respectively. As shown in Figure 3, the CV values in the transmission images processed with the ANLG filter were smaller than those in the images processed with the NLG filter. Furthermore, the CV values decreased with increasing transmission scan time, but increased with increasing diameter of the phantom in both cases. The scattered radiation increases with increasing diameter of the phantom, leading to an increase of statistical noise. Thus, the CV values in the transmission images are considered to increase with increasing diameter of the phantom. However, when using the ANLG filter, their dependency on the transmission scan time and phantom size was smaller than when using the NLG filter.

Figure 4 shows the CV values in the transmission images of the pool phantom with various injected doses of ^{18}F-FDG as a function of transmission scan time. Figures 4 (a) and 4 (b) show cases when using the NLG and ANLG filters, respectively. As shown in Figure 4, the CV values in the transmission images processed with the ANLG filter were smaller than those in the images processed with the NLG filter. Furthermore, the CV values in the transmission images increased with increasing injected dose in both cases. This appears to be mainly due to the fact that the scattered radiation increases with increasing injected dose, leading to an increase of statistical noise. However, when using the ANLG filter, their dependency on the injected dose of ^{18}F-FDG was smaller than when using the NLG filter.

Figures 5 and 6 show examples of the transmission images of the pool phantom processed with the NLG and ANLG filters and their emission images, respectively, as a function of transmission scan time. The upper and lower panels in Figures 5 and 6 show cases when using the NLG and ANLG filters, respectively. In these cases, the diameter of the phantom and the injected dose of ^{18}F-FDG were 20 cm and 111 MBq, respectively. Visual comparison in Figures 5 and 6 demonstrated that the ANLG filter was more effective for noise reduction than the NLG filter, not only in the transmission images but also in the emission images, especially for short transmission scan time.

Clinical study

Figures 7 (a) and 7 (b) show the CV values in the liver region in the emission images of two volunteers A and B as a function of transmission scan time. As shown in Figure 7, the CV values in the images processed with the

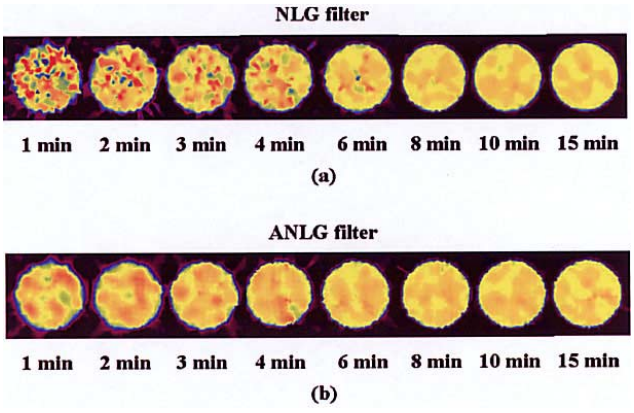

Fig. 5 Transmission images of the pool phantom processed with the NLG (a) and ANLG filters (b) for various transmission scan times. The diameter of the phantom and the injected dose of ^{18}F-FDG were 20 cm and 111 MBq, respectively.

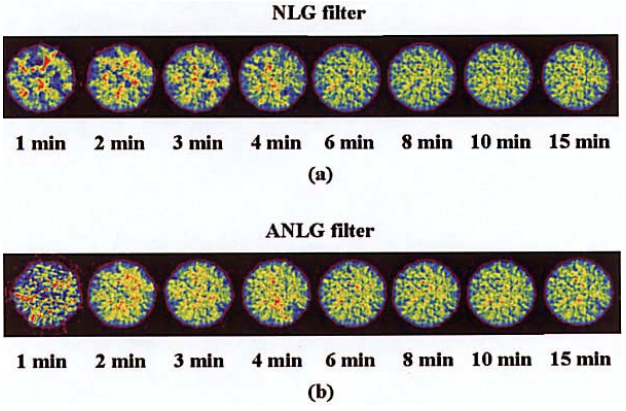

Fig. 6 Emission images of the phantom from Figure 4 in which the transmission images were processed with the NLG (a) and ANLG filters (b) for various transmission scan times.

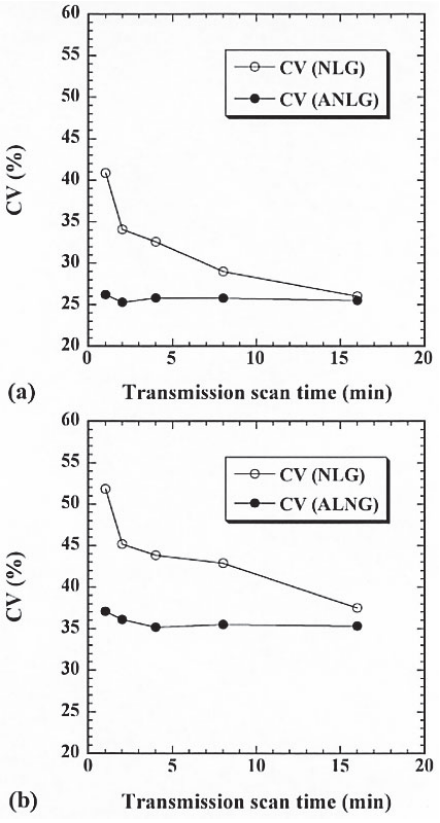

Fig. 7 CV values in the emission images of two volunteers in whom the transmission images were processed with the NLG (*open circles*) and ANLG filters (*closed circles*) as a function of transmission scan time. (a) for a volunteer with a body mass index (BMI) of 20.2 (volunteer A) and (b) for a volunteer with a BMI of 25.3 (volunteer B).

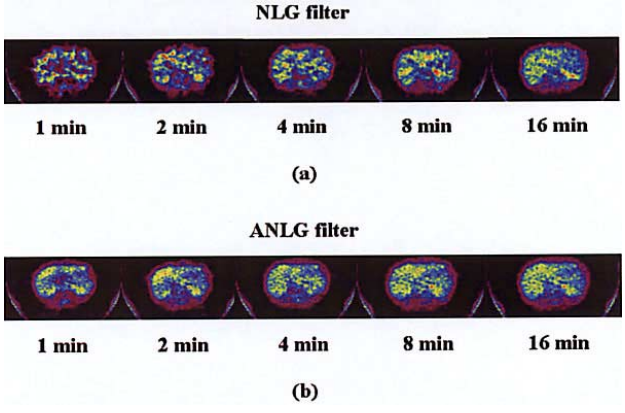

Fig. 8 Emission images of volunteer A in whom the transmission images were processed with the NLG (a) and ANLG filters (b) for various transmission scan times.

ANLG filter were smaller than those in the images processed with the NLG filter. Furthermore, when using the ANLG filter, the CV values remained almost constant regardless of the transmission scan time, while they largely varied depending on the transmission scan time when using the NLG filter. As shown in Figures 7 (a) and 7 (b), the CV value in the image of volunteer A was smaller than that of volunteer B. This would be due to the difference in the amount of scattered radiation.

Figures 8 (a) and 8 (b) show the emission images of volunteer A in which the transmission images were processed with the NLG and ANLG filters, respectively, for various transmission scan times. Visual comparison demonstrated that the ANLG filter was more effective for noise reduction than the NLG filter. Furthermore, the shape of the liver was more visible in the image processed with the ANLG filter than that in the image processed with the NLG filter especially at the short transmission scan time. This indicates that the ANLG filter reduces the statistical noise while maintaining the structural information. Thus, the ANLG filter also appears to be effective for the improvement of spatial resolution.

Figures 9 (a) and 9 (b) show the correlation and Bland-Altman plot[11] between SUV [NLG (7 min)] and SUV

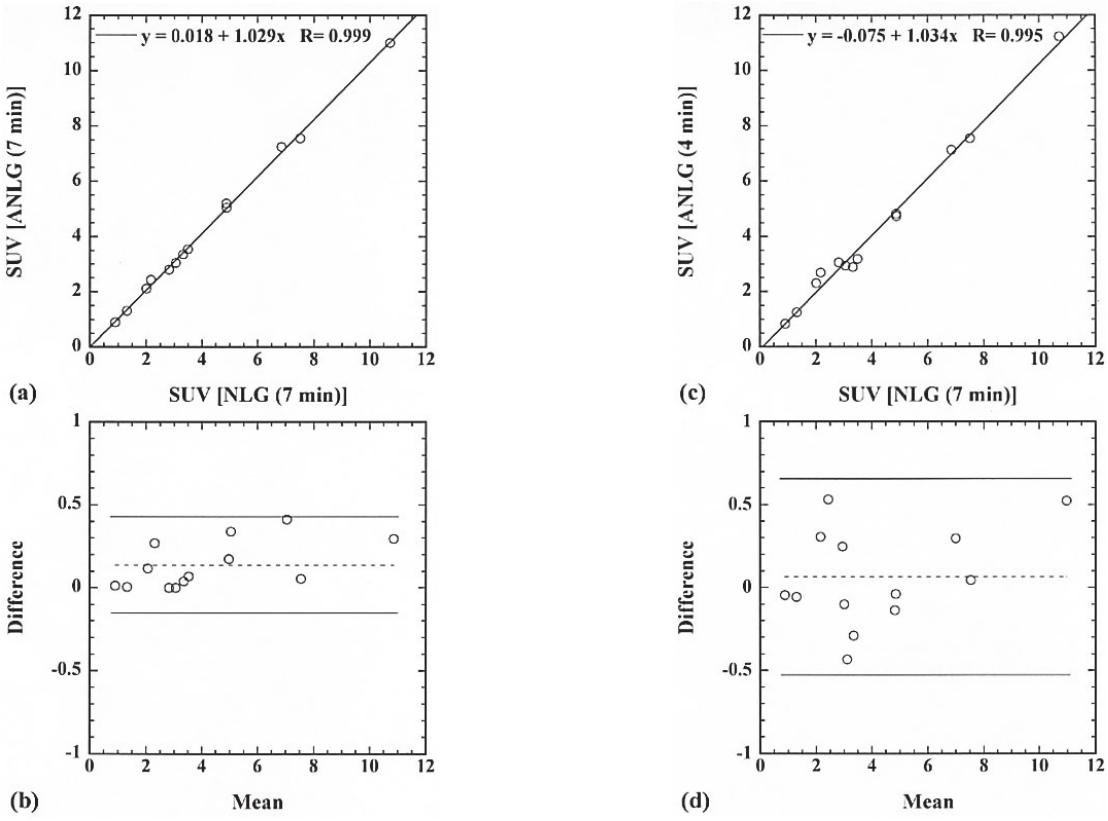

Fig. 9 Correlation [(a) and (c)] and Bland-Altman plot [(b) and (d)] between the standardized uptake values (SUVs) obtained from the emission images in which the transmission image was processed using the NLG and ANLG filters. (a) and (b) show the correlation and Bland-Altman plot between SUV [NLG (7 min)] and SUV [ANLG (7 min)], respectively, while (c) and (d) show those between SUV [NLG (7 min)] and SUV [ANLG (4 min)], respectively. In these figures, SUV [NLG (7 min)] represents the SUV obtained from the emission image in which the transmission image with a scan time of 7 min was processed using the NLG filter. SUV [ANLG (7 min)] and SUV [ANLG (4 min)] represent the SUV obtained from the emission images in which the transmission image was processed using the ANLG filter and the transmission scan time was taken as 7 min and 4 min, respectively.

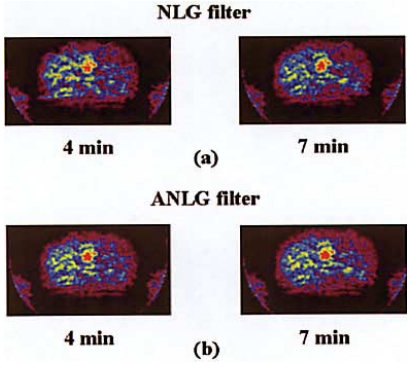

Fig. 10 Emission images of a patient with a tumor (patient No. 9 in Table 1) in whom the transmission images were processed with the NLG (a) and ANLG filters (b). The left and right panels show cases when the transmission scan time was taken as 4 min and 7 min, respectively.

[ANLG (7 min)], respectively, while Figures 9 (c) and 9 (d) show those between SUV [NLG (7 min)] and SUV [ANLG (4 min)]. As shown in Figure 9 (a), there was an excellent correlation between SUV [NLG (7 min)] and SUV [ANLG (7 min)] ($r = 0.999$ and $y = 1.029x + 0.018$). The differences between them were within mean ± 2SD as shown in the Bland-Altman plot [Fig. 9 (b)]. There was also an excellent correlation between SUV [NLG (7 min)] and SUV [ANLG (4 min)] ($r = 0.995$ and $y = 1.034x - 0.075$) [Fig. 9 (c)]. The differences between them were also within mean ± 2SD as shown in the Bland-Altman plot [Fig. 9 (d)].

Figures 10 (a) and 10 (b) show the emission images of a patient (patient No. 9 in Table 1) in whom the transmission images were processed with the NLG and ANLG filters, respectively. The left and right panels show cases when the transmission scan time was taken as 4 min and 7 min, respectively. As shown in Figure 10, when using the NLG filter, there was a large difference in image quality between the transmission scan times of 4 min and

7 min. On the other hand, when using the ANLG filter, the image quality when the transmission scan time was taken as 4 min was almost equal to that when the transmission scan time was taken as 7 min.

DISCUSSION

Kitamura et al.[4] applied the NLG filter to smoothing transmission images reconstructed using the FBP method instead of using iterative reconstruction and segmentation methods, and concluded that the NLG filtering method is useful for attenuation correction using count-limited transmission data for both brain and whole-body PET studies. However, we have sometimes experienced that the NLG filter is not sufficient for noise reduction especially when the transmission scan time is short. This is considered to be due to the fact that the smoothing parameters g and h in the NLG filter operation [Eq. (2)] are determined irrespective of the noise extent of the targeted image. To overcome this drawback, Kitamura[5] developed the ANLG filter by modifying the NLG filter such that the smoothing parameters g and h are varied depending on the noise variance individually estimated from the measured transmission sinograms [Eq. (6)]. We applied the NLG and ANLG filters to transmission images, and evaluated the usefulness of the ANLG filter in comparison with that of the NLG filter using phantom and clinical studies especially when the transmission scan time was short.

The present study demonstrated that the ANLG filter can effectively reduce the statistical noise in transmission images even for short transmission scan times and is an effective way to reduce the propagation of the statistical noise in transmission data into emission data without the loss of quantitative accuracy of FDG-PET studies.

As shown in Figures 3, 4 and 7, the CV values in the transmission images processed with the ANLG filter were lower than those in the images processed with the NLG filter in phantom and clinical studies, indicating that the ANLG filter is more effective for noise reduction than the NLG filter especially with short transmission scan times. Visual comparison of the transmission and emission images (Figs. 5, 6 and 8) also confirmed these results. Furthermore, the SUVs in the emission images reconstructed using the transmission images with a scan time of 4 min and processed with the ANLG filter showed excellent correlations with those in the images reconstructed using the transmission images with a scan time of 7 min and processed with the NLG filter (Fig. 9), suggesting that the ANLG filter can shorten the time needed for FDG-PET studies without deteriorating their quantitative accuracy.

The present study also demonstrated that the capability of noise reduction of the ANLG filter evaluated in terms of CV values was less sensitive to the phantom size, injected dose of ^{18}F-FDG and transmission scan time than that of the NLG filter (Figs. 3, 4 and 7). This appears to be due to the fact that the adjustable parameters in the ANLG filter [g and h in Eq. (2)] are effectively adapted to the noise variance of the targeted image. This aspect of the ANLG filter will be useful especially in routine clinical settings in which patients with various body sizes and injected doses of ^{18}F-FDG should be studied.

Several segmentation methods have been proposed,[12–14] assigning uniform attenuation coefficients into segmented regions of transmission images. However, these methods usually require a priori assumptions with respect to the number of anatomic groups and can cause classification errors when the count statistics of transmission data are very poor. Recently, iterative reconstruction methods using Bayesian priors have been proposed[15,16] as an alternative to FBP reconstruction. Although these reconstruction methods can remove noise without blurring edges in transmission images, they need very long calculation times especially in the case of whole-body PET studies.

In contrast to some segmentation methods,[12–14] the ANLG filtering method presented here is faster than the iterative reconstruction methods and the smoothing parameters can be automatically determined. With segmentation methods, transmission images are generally segmented into regions (clusters) of known attenuation coefficients such as lungs, soft tissue, bone and air.[17] If there are some regions such as a bed and head holder except for the above regions, these regions should be processed separately from the above regions.[17] The final attenuation coefficient map is then calculated by combining the segmented and original images in a weighted fashion, followed by adding up a separately processed image such as the bed and head holder images.[17] On the other hand, with the ANLG filtering method, there is no need to separately process the regions such as a bed and head holder in the transmission images. This method can also deal with the large variability of attenuation values in the lungs and make attenuation correction factors more specific to the study like in the NLG filtering method.[4] Together with short transmission scans or simultaneous emission and transmission scans,[9,10] this method will make quantitative PET studies more feasible and increase patient throughput.

As previously described, we extracted transmission data by separating the transmission and emission data from SET data in this study, and investigated the usefulness of the ANLG filter in comparison with the NLG filter by using the transmission data thus obtained. Therefore, it also appears to be necessary to investigate the case when the transmission and emission data are acquired separately. This investigation will be the subject of a future study.

In this study, we performed attenuation correction using transmission data in FDG-PET studies, and attempted to improve the quality of the transmission data using the ANLG filter. Recently, however, combined

PET and computed tomography (CT) (PET/CT) scanners have been developed that enable coregistered PET and CT images to be acquired in quick succession[18] and have been increasingly used clinically. With PET/CT scanners, attenuation coefficient maps for 511-keV γ ray can be generated from CT images to correct for attenuation in PET emission data. Although a comparison between the transmission-based and CT-based attenuation correction methods is beyond the scope of the purpose of the present study, this will also be the subject of a future study.

CONCLUSION

This study suggests that the ANLG filter is effective and useful for noise reduction in transmission images and shortening transmission scan time while maintaining the quantitative accuracy of FDG-PET studies.

REFERENCES

1. Gambhir SS, Czernin J, Schwimmer J, Silverman DH, Coleman RE, Phelps ME. A tabulated summary of the FDG-PET literature. *J Nucl Med* 2001; 42: 1S–93S.
2. Aurich V, Weule J. Non-linear Gaussian filters performing edge preserving diffusion. In *Proceedings 17. DAGM-Symposium*, Bielefeld; Springer, 1995: 538–545.
3. Winkler G, Aurich V, Hahn K, Martin A, Rodenacker K. Noise reduction in images: some recent edge-preserving methods. Technical Report 98-15, Institute of Biomathematics and Biometrics, GSF-National Research Center for Environment and Health, Neuherberg, Germany, December 1998. (This report can be downloaded from http://www.gsf.de/ibb.)
4. Kitamura K, Iida H, Shidahara M, Miura S, Kanno I. Noise reduction in PET attenuation correction using non-linear Gaussian filters. *IEEE Trans Nucl Sci* 2000; 47: 994–999.
5. Kitamura K. Investigation of Methods for High-throughput Positron Emission Tomography, PhD Dissertation, Osaka University, 2003.
6. Harpen MD. A simple theorem relating noise and patient dose in computed tomography. *Med Phys* 1999; 26: 2231–2234.
7. Shepp LA, Logan BF. The Fourier reconstruction of a head section. *IEEE Trans Nucl Sci* 1974; NS-21: 21–43.
8. Hudson HM, Larkin R. Accelerated image reconstruction using ordered subsets of projection data. *IEEE Trans Med Imag* 1994; 13: 601–609.
9. Meikle SR, Bailey DL, Hooper PK, Eberl S, Hutton BF, Jones WF, et al. Simultaneous emission and transmission measurements for attenuation correction in whole-body PET. *J Nucl Med* 1995; 36: 1680–1688.
10. Inoue T, Oriuchi N, Kunio M, Tomiyoshi K, Tomaru Y, Aoyagi K, et al. Accuracy of standardized value uptake measured by simultaneous emission and transmission scanning in PET oncology. *Nucl Med Commun* 1999; 20: 849–857.
11. Bland JM, Altman DG. Statistical methods for assessing agreement between two methods of clinical measurement. *Lancet* 1986; 1: 307–310.
12. Xu Z, Mullani NA, Gould KL, Anderson WL. A segmented attenuation correction for PET. *J Nucl Med* 1991; 32: 161–168.
13. Meikle SR, Dahlbom M, Cherry SR. Attenuation correction using count-limited transmission data in positron emission tomography. *J Nucl Med* 1993; 34: 143–150.
14. Xu M, Cutler PD, Luk WK. Adaptive segmented attenuation correction for whole-body PET imaging. *IEEE Trans Nucl Sci* 1996; 43: 331–336.
15. Mumcuoglu EU, Leahy R, Cherry S, Zhou Z. Fast gradient-based methods for Bayesian reconstruction of transmission and emission PET images. *IEEE Trans Med Imag* 1994; 13: 687–701.
16. Fessler JA, Ficaro EP, Clinthorne NH, Lange K. Grouped coordinate ascent algorithms for penalized-likelihood transmission image reconstruction. *IEEE Trans Med Imag* 1997; 16: 166–175.
17. Zaidi H, Diaz-Gomez M, Boundraa A, Slosman DO. Fuzzy clustering-based segmented attenuation correction in whole-body PET imaging. *Phys Med Biol* 2002; 47: 1143–1160.
18. Beyer T, Townsend DW, Brun T, Kinahan PE, Charron M, Roddy R, et al. A combined PET/CT scanner for clinical oncology. *J Nucl Med* 2000; 41: 1369–1379.